

Effects of Low Molecular Weight Compounds with Hydroxyl Groups on Properties of Poly(L-lactic acid)

YONG HE, NAOKI ASAKAWA, JIANCHUN LI, YOSHIO INOUE*

Department of Biomolecular Engineering, Tokyo Institute of Technology, Nagatsuta 4259, Midori-Ku, Yokohama 226-8501, Japan

Received 24 July 2000; accepted 5 December 2000

ABSTRACT: The effects of low molecular weight compounds with hydroxyl groups on the properties of poly(L-lactic acid) (PLLA) were investigated. The specific interaction between PLLA and 4,4'-thiodiphenol (TDP) was investigated by Fourier transform IR spectroscopy. The spectra of the blends suggested that there were interassociated hydrogen bonds between the PLLA chains and TDP molecules. The thermal and dynamic mechanical properties of PLLA/TDP blends were investigated by differential scanning calorimetry and dynamic mechanical thermal analysis, respectively. The results revealed that the thermal and dynamic mechanical properties of PLLA were greatly modified through blending with TDP and that PLLA/TDP blends possessed eutectic phase behavior. The effects of the thermal history on the formation of hydrogen bonds and the thermal and mechanical properties were evaluated. It was found that the properties of the blends were strongly dependent on the thermal history. In addition to TDP, PLLA blends with other low molecular weight hydroxyl compounds, including aromatic and aliphatic compounds, were also characterized. The effects of the chemical structure of the low molecular weight compounds on the properties of PLLA were discussed. © 2001 John Wiley & Sons, Inc. *J Appl Polym Sci* 82: 640–649, 2001

Key words: poly(L-lactic acid); 4,4'-thiodiphenol; hydrogen bond; Fourier transform IR spectroscopy

INTRODUCTION

Poly(L-lactic acid) (PLLA) is a hydrolysable, biocompatible, and ecologically safe thermoplastic, which can be commercially produced from renewable resources.¹ It has been investigated as a material for controlled-release devices,² absorbable sutures and fibers,^{3,4} and implants for bone fixation.⁵ Currently, there is increasing interest in using PLLA for disposable biodegradable plastic articles.⁶

In order to modify the properties, PLLA was blended with a number of polymers such as poly(glycolic acid),⁷ poly(ethylene vinyl acetate),⁸ poly(4-vinylphenol),⁹ poly(ϵ -caprolactone),^{10,11} poly(3-hydroxybutyrate),¹² and poly(ethylene oxide).¹³ Recently, PLLA was also blended with low molecular weight compounds of citrate esters.¹⁴ The citrate esters were found to be effective in lowering the glass-transition temperature and improving the elongation at break.¹⁴ Moreover, the hydrolytic and enzymatic degradation of PLLA was suggested to be controllable through blending with the citrate esters.¹⁴

In this investigation an effort was made to study the effect of low molecular weight dihydric phenols on the thermal and mechanical proper-

Correspondence to: Y. Inoue (yinoe@bio.titech.ac.jp).

Contract grant sponsor: Ministry of Education, Science, Sports and Culture, Japan; contract grant number: 11217204(2000).

Journal of Applied Polymer Science, Vol. 82, 640–649 (2001)
© 2001 John Wiley & Sons, Inc.

ties of PLLA. Nowadays, a variety of low molecular weight additives, such as fillers, antioxidants, and plasticizers, are included in polymer materials in industry to modify their properties and greatly widen their application field. Wu et al. recently reported that dihydric phenol can greatly improve the damping properties of polymer materials.¹⁵ In a previous work, we also found that the addition of 4,4'-thiodiphenol (TDP) to poly(ϵ -caprolactone) is an effective way to modify the thermal and mechanical properties of the polyester.¹⁶ On the other hand, dihydric phenol possesses the potential ability to form strong intermolecular hydrogen bonds with carbonyl, ether, or other functional groups. We found that the two hydroxy groups in a molecule of dihydric phenol could form two hydrogen bonds at the same time with two carbonyl groups of different polymer chains.¹⁶ We expect that dihydric phenol could be used as a compatibilizer to improve the miscibility between the immiscible polymer pairs through the formation of intermolecular hydrogen bonds.

This work focuses on the interassociated hydrogen bond between PLLA and TDP with the employment of Fourier transform IR spectroscopy (FTIR). The relationship between this specific interaction and the thermal and dynamic mechanical properties of the blends, as determined by differential scanning calorimetry (DSC) and dynamic mechanical thermal analysis (DMTA), are elucidated.

EXPERIMENTAL

Materials

The PLLA sample (LACEA®; $M_w = 1.33 \times 10^5$, $M_w/M_n = 1.70$) was supplied by Mitsui Chemical Co. The TDP, 4,4'-dihydroxydiphenylmethane (DPM), catechol (CAT), 1,4-dihydroxybenzene (DHB), 1,4-di-(2-hydroxyethoxy) benzene (DHEB), and 1,6-hexanediol (HDO) were purchased from Tokyo Kasei Kogyo Co. All the reagents were used as received.

Blend Preparation

The PLLA and TDP in appropriate weight ratios were first dissolved in chloroform/1,4-dioxane (80/20, v/v). Then the solution was cast on a glass petri dish and the solvent was evaporated at room temperature overnight. All the resultant films were placed in an oven at 60°C under a vacuum

for 2 days to remove the residual solvent. The casting films were subsequently compression molded between Teflon sheets for 3 min at 190°C and under a pressure of 5 MPa with a Toyoseiki laboratory press (Mini Test Press-10). This was followed by a fast cooling to room temperature between two iron plates. The hot-pressed films were used for thermal analysis and tensile tests after annealing at 70°C for 1 week or aged at room temperature for 2 months.

The films of PLLA blends with DPM, CAT, DHB, DHEB, and HDO were prepared by casting from the chloroform/1,4-dioxane (80/20, v/v) solution. After the solvent was evaporated, the casting films were aged at 70°C for more than 1 week before the thermal analysis.

In order to indicate the different contents of the blends, the following codes were used: LATDP10, LATDP20, LATDP30, and so on, where LATDP refers to PLLA/TDP blends and the numbers refer to the TDP weight content in the blends.

FTIR Measurements

Films of the blends with a thickness suitable for FTIR measurements were prepared by dropping the polymer blend solution on the surface of a silicon wafer. The silicon wafer was transparent for the IR incident beam and was used as the substrate. The thickness of the casting film was carefully controlled to be thin enough to ensure that the studied absorption was within the linearity range of the IR detector. After drying under a vacuum for 2 days, the samples were melted at 190°C for 4 min followed with a fast cooling to room temperature. Then the samples were aged at room temperature or 70°C for 1 week before the measurements.

The IR measurements were carried out on a single-beam IR spectrometer (Perkin-Elmer Spectra 2000). All spectra were recorded under a resolution of 4 cm^{-1} and an accumulation of 16 scans.

DSC Testing

The DSC thermogram of the sample (about 5 mg), which was presealed in aluminum pans, was recorded on a Seiko DSC 220 system. The samples were first heated from -60 to 200°C at a heating rate of 20°C/min (the first heating scan). After that the samples were rapidly quenched to -100°C with liquid nitrogen and then reheated to 200°C at a rate of 20°C/min (the second heating

scan). The melting temperature (T_m) was determined from the maximum of the DSC endothermic peak. The value of the melting enthalpy (ΔH) was calculated as the integral of the endothermic peak in the DSC curve. The glass-transition temperature (T_g) was taken as the peak top of the differentiation of DSC curve obtained from the second heating scan.

DMTA Measurements

Dynamic mechanical spectra were recorded on a Seiko-DMS210 instrument under the tensile mode at 5 Hz and a thermal scanning rate of 2°C/min. The test samples had lengths of 30 mm, widths of 8 mm, and thicknesses of about 200 μm . Before the analysis, the test samples prepared by a hot press were annealed at 70°C for 1 week.

Tensile Tests

Dumbbell-shaped specimens were cut from hot-pressed films with a thickness of about 200 μm and were used for the tensile measurements. Stress-strain curves were recorded on an EZTest tensile tester (Shimadzu Co.) at room temperature with a crosshead speed of 5 mm/min. The modulus, stress, and strain were determined from these curves and averaged over 5–10 specimens.

RESULTS AND DISCUSSION

Hydrogen Bonds between PLLA and TDP

FTIR spectroscopy is a particularly suitable technique for investigating specific intermolecular interactions. The PLLA blends studied here contained a carbonyl group and yielded a $\nu_{\text{C=O}}$ stretching mode at about 1759 cm^{-1} , while TDP showed no absorption in the region ranging from 1690 to 1810 cm^{-1} . Hence, any change of the FTIR spectrum in this region should be attributed to change in the carbonyl group environment, such as the formation of hydrogen bonds.

Two kinds of blend samples with different thermal histories were characterized by FTIR spectroscopy: samples aged at room temperature for 1 week, and samples annealed at 70°C for 1 week. For the samples aged at room temperature for 1 week the FTIR spectra in the carbonyl vibration region are displayed in Figure 1 as a function of the TDP composition. The carbonyl vibration band of the PLLA component showed a tendency to shift to a low wave number after blending with

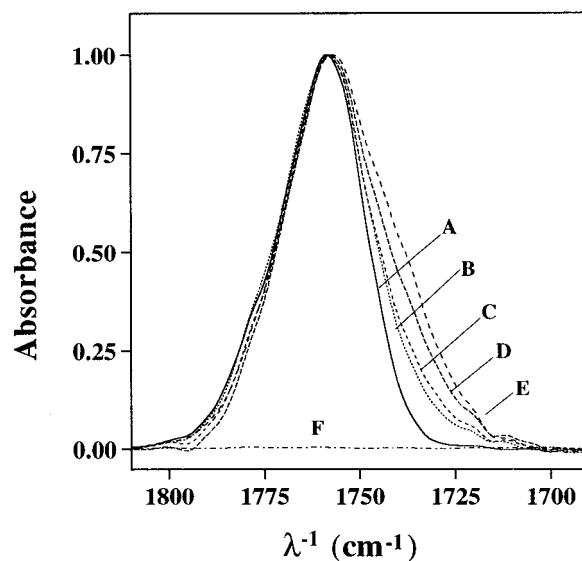


Figure 1 The normalized FTIR spectra in the carbonyl vibration region of pure PLLA, TDP, and their blends with TDP contents from 10 to 40 wt %. The samples were aged at room temperature for 1 week. PLLA (spectrum A), LATDP10 (spectrum B), LATDP20 (spectrum C), LATDP30 (spectrum D), LATDP40 (spectrum E), and TDP (spectrum F).

TDP; the peak wave number for PLLA was 1759 cm^{-1} while that for LATDP40 was 1757 cm^{-1} . Furthermore, it can be clearly seen that the vibration band became broader with the increase of TDP content in the blend; the peak widths at half-height for PLLA and the LATDP40 blend were 25.4 and 34.1 cm^{-1} , respectively. The difference between the FTIR spectrum of pure PLLA and that of the PLLA/TDP blend should be attributed to the appearance of the hydrogen-bonded carbonyl vibration band in the spectrum of the blend, and it indicated the formation of intermolecular hydrogen bonds between the polyester and TDP molecules.

The interassociated carbonyl vibration band can be extracted by subtracting the “free” carbonyl vibration band from the carbonyl vibration bands of the blend. As an example, Figure 2 shows the hydrogen-bonded carbonyl vibration band of LATDP40 obtained by subtracting the spectrum of pure PLLA from that of the LATDP40 blend. It can be seen that the vibration band of the interassociated carbonyl groups is centered at 1739 cm^{-1} . By integrating the respective areas of the contributions due to the hydrogen-bonded and free carbonyl groups, the fractions of the interassociated carbonyl groups (F_b) can be estimated from eq. (1):¹⁷

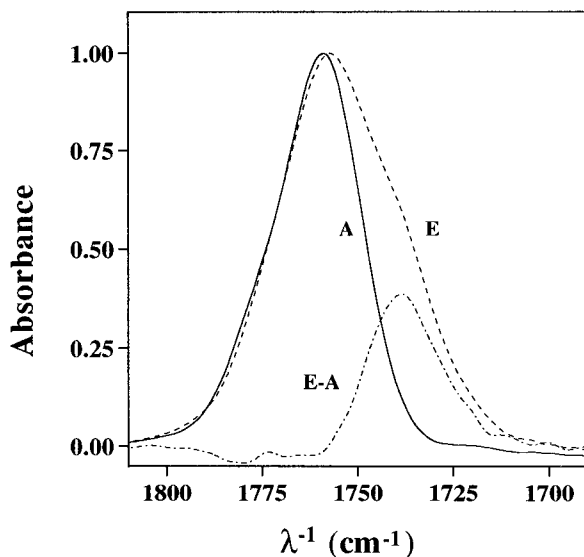


Figure 2 The FTIR spectra in the carbonyl vibration region of pure PLLA (spectrum A), the LATDP40 (spectrum E) blend, and their difference spectrum (E - A). The samples were aged at room temperature for 1 week.

$$F_b = A_b / (A_b + \gamma A_f) \quad (1)$$

where A_b and A_f are the areas corresponding to the hydrogen-bonded and free carbonyl groups vibrations, respectively, and γ is the absorption ratio that takes into account the difference between the absorptivities of the hydrogen-bonded and free carbonyl groups. Taking a γ value of 1.5, which is comparable to the published data for similar systems,¹⁸⁻²⁰ the fractions of the F_b were calculated and are plotted in Figure 3 as a function of composition. Obviously, the F_b increased with the increase of TDP content in the blend.

Figure 4 shows the FTIR spectra of PLLA/TDP blends (aged at room temperature for 1 week) in the hydroxyl stretching region, which is also a region of interest because of the involvement of hydroxyl groups in hydrogen bonding. In the hydroxy vibration region of pure TDP, three vibration bands appeared that were centered at 3318, 3265, and 3183 cm^{-1} . These bands should be assigned to self-associated hydroxyl groups in pure TDP, because their wave numbers were low. For pure PLLA only very weak bands (at about 3510 cm^{-1}) were observed in this region, which should be attributed to the vibration of the hydroxy group in the terminal chain of PLLA. Because of its low intensity compared to the bands of TDP in this vibration region, the contribution of this

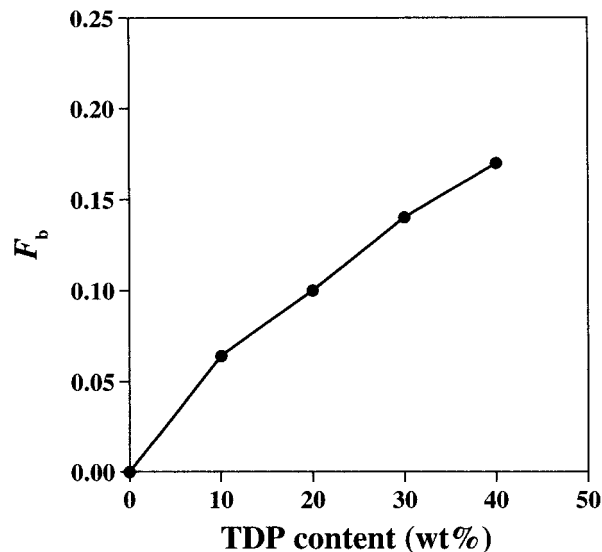


Figure 3 The fractions of the interassociated carbonyl groups (F_b) in the PLLA/TDP blends aged at room temperature for 1 week.

band to the spectra of blends should have been negligible when the content of TDP was not too low. In the spectra of PLLA/TDP blends the bands shifted to a high wave number (about 3484 cm^{-1}) compared to that of pure TDP, indicating that the

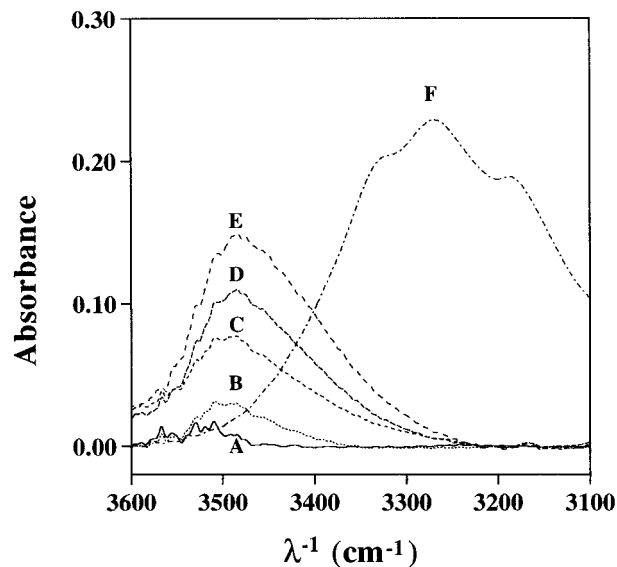


Figure 4 The FTIR spectra in the hydroxyl vibration region of pure PLLA, TDP, and their blends with TDP contents from 10 to 40 wt %. The samples were aged at room temperature for 1 week. PLLA (spectrum A), LATDP10 (spectrum B), LATDP20 (spectrum C), LATDP30 (spectrum D), LATDP40 (spectrum E), and TDP (spectrum F).

interassociated hydrogen bonds were weaker than the self-associated ones.

For the samples annealed at 70°C for 1 week, there was little change between the FTIR carbonyl vibration region of pure PLLA and that of the PLLA/TDP blend. As an example, the FTIR carbonyl vibration bands of PLLA and the LATDP40 blend are compared in Figure 5. Figure 6 shows that the wave number of the hydroxyl vibration bands in the LATDP40 blend (aged at 70°C) was almost the same as that in pure TDP. These results suggested that no interassociated hydrogen bond or no strong interassociated hydrogen bond was retained in the PLLA/TDP blends after annealing at 70°C for 1 week. The annealing should prompt the crystallization of PLLA and TDP. Then the crystallization should facilitate the separation of TDP from PLLA. As a result, the interassociated hydrogen bond or strong interassociated hydrogen bond disappeared.

Thermal and Dynamic Mechanical Properties

The DSC analysis was performed to study the thermal behavior of the blends. Figure 7 shows the DSC traces of PLLA/TDP blends (annealed at 70°C for 1 week) with various TDP contents recorded at the first heating scan. Obviously, the

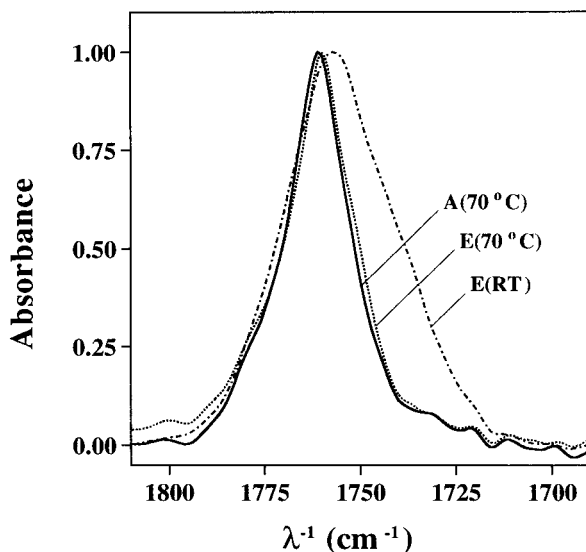


Figure 5 The normalized FTIR spectra in the carbonyl vibration region for pure PLLA (spectrum A), LATDP40 (spectrum E) blend aged at 70°C for 1 week. The spectrum of the LATDP40 blend [spectrum E(RT)] aged at room temperature for 1 week is also shown for comparison.

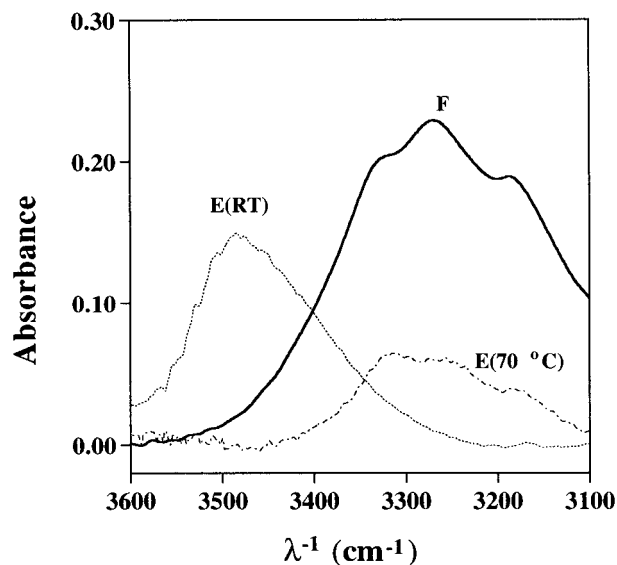


Figure 6 The FTIR spectra in the hydroxyl vibration region for pure TDP (spectrum F) and the LATDP40 blend aged at 70°C for 1 week [spectrum E(70 °C)]. The spectrum of the LATDP40 blend aged at room temperature for 1 week [E(RT)] is also shown for comparison.

melting point of PLLA dropped drastically with the increase of TDP content when the TDP content was not too high.

Only one melting peak appeared in the DSC trace of the pure component. Two melting points were observed for most of the blends. The higher melting point decreased with the increase of the TDP content at low TDP content while it increased with the TDP content at high TDP content. The lower melting point appeared to be independent of the blend composition and was therefore likely to be attributed to the melting of a eutectic mixture.

The phase diagram of PLLA/TDP blends (Fig. 8) was constructed based on the following interpretation of the DSC melting endotherm.^{21–23} When the eutectic melting occurs, either in eutectic or off-eutectic mixtures, the peak temperature of the relatively sharp endotherm is used to construct a composition-independent isothermal phase boundary representing three-phase (solid–solid–liquid) equilibria. When composition-dependent melting occurs over a rather broad temperature range above the eutectic endotherm in off-eutectic mixtures, the end point of this asymmetric melting event is used to construct the liquidus phase boundary that separates the solid–liquid two-phase regions from the homogeneous state. For pure components, the end point of the relatively sharp endothermic transition is chosen.

The phase diagram of PLLA/TDP blends (Fig. 8) has the characteristics of a eutectic system. The melting temperature of the eutectic mixture was about 115°C. The content of TDP at the eutectic point (42 wt %) was determined from the composition at which the eutectic melting heat was at maximum.²³

The melting enthalpy of PLLA/TDP blends versus the content of TDP is plotted in Figure 9. The dotted line expresses the sum of the melting enthalpies of the two components in the pure state. It is clear that the values of the melting enthalpy for PLLA/TDP blends fell below the dotted line, indicating that the crystallinity of at least one component decreased after blending.

The DSC thermograms in the second heating scan are summarized in Figure 10 for PLLA/TDP blends. Both the crystallization peak and melting peak were observed in the DSC curves of pure PLLA, LATDP50 blends, and LATDP60 blends. The crystallization peaks of LATDP50 and LATDP60 blends should contribute to the crystal-

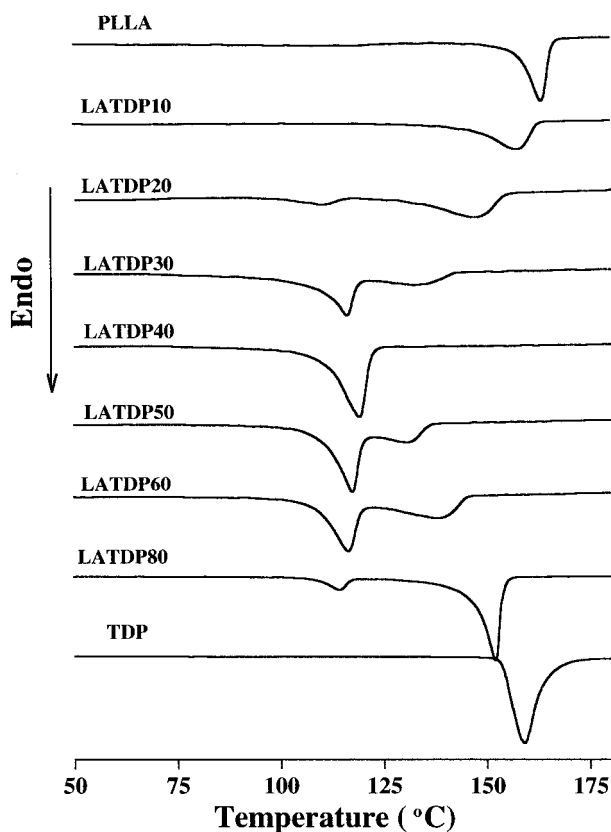


Figure 7 The DSC traces in the first heating scan of pure PLLA, TDP, and their blends with various TDP contents. Before analysis, the samples were annealed at 70°C for 1 week.

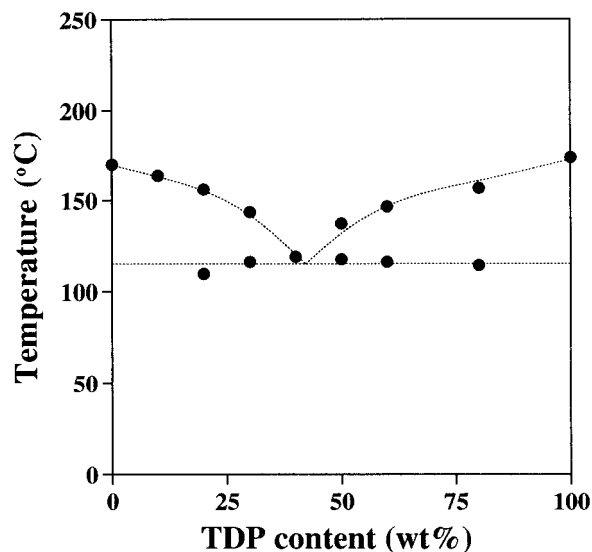


Figure 8 The phase diagram of PLLA/TDP blends.

lization of the TDP component rather than that of the PLLA component. By contrast, neither a crystallization peak nor a melting peak was observed in the thermograms of the blends with TDP contents from 10 to 40 wt %. These facts should suggest that the cold crystallization of the PLLA component in the blend was completely inhibited under the experimental conditions.

From Figure 10 it can also be observed that the glass-transition temperatures (T_g) of the blend dropped drastically with the increase of TDP content. The relationship between the T_g and TDP

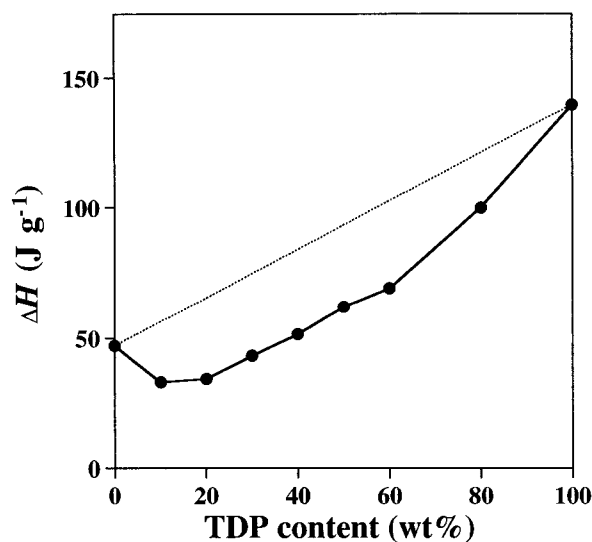


Figure 9 The melting enthalpy of the PLLA/TDP blend annealed at 70°C for 1 week.

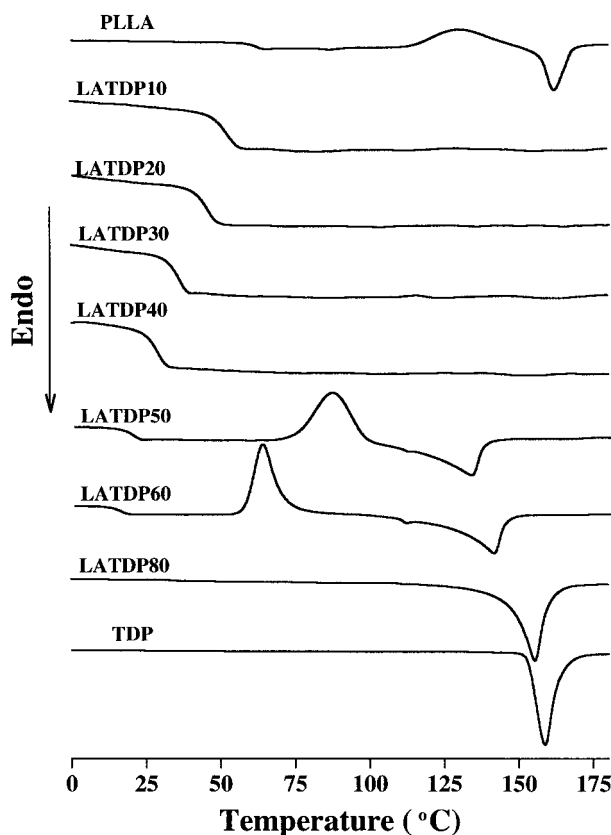


Figure 10 The DSC traces of pure PLLA, TDP, and their blends with various TDP contents recorded at the second heating scan.

content is depicted in Figure 11 for the blends. Clearly, the change of the T_g (determined from DSC) with the TDP content followed a linear relationship rather well. This result strongly suggested that PLLA and TDP were miscible in the melting state. Extrapolating the line to a TDP content of 100 wt %, a T_g of -17.7°C was estimated for pure TDP.

The thermal behavior of the sample aged at room temperature for 2 months was evidently different from that of the sample annealed at 70°C for 1 week. Table I summarizes the melting temperatures and enthalpies of the samples aged under different conditions. The melting enthalpy of the sample aged at room temperature was much lower than that of the sample annealed at 70°C .

The crystallization of the blend should be directly related to the interassociated hydrogen bonds. The presence of hydrogen bonds should hinder the crystallization of the PLLA and TDP component, which was evident from the melting enthalpies. On the other hand, the crystallization

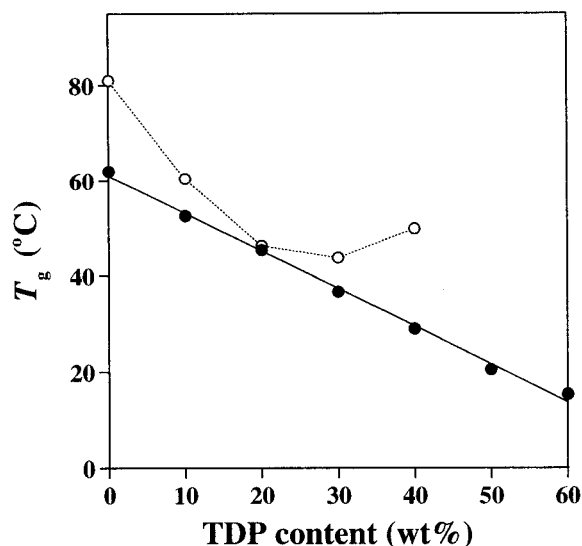


Figure 11 The relationship between the glass-transition temperature (T_g) and TDP content for PLLA/TDP blends. The T_g was determined from the measurements of (●) DSC and (○) DMTA.

led to the phase separation and then parts of the interassociated hydrogen bond disappeared.

Figures 12 and 13 depict the dynamic mechanical spectra of PLLA and the blends with TDP contents from 10 to 40 wt %. At low temperature (below 30°C) the storage modulus (E') of PLLA/TDP blends was larger than that of pure PLLA (Fig. 12). However, the storage modulus of the blend was basically lower than that of pure PLLA at high temperature (over 50°C ; Fig. 12). From Figure 13 two differences can be noted in the relaxation behavior between pure PLLA and the blends: the α -transition peak became broad, and the value of the $\tan(\delta)$ on the peak top decreased with the increase of TDP content. These differences may be related to the change of phase structure after the incorporation of TDP.

Table I Melting Point (T_m) and Melting Enthalpy (ΔH) for PLLA/TDP Samples Aged at 70°C or Room Temperature (RT)

Sample	70°C for 1 Week		RT for 2 Months	
	T_m ($^\circ\text{C}$)	ΔH	T_m ($^\circ\text{C}$)	ΔH
PLLA	164	47.1	164	17.5
LATDP10	155	33.1	154	3.7
LATDP20	110, 145	34.4	93, 143	6.4
LATDP30	116, 133	43.3	93	11.1

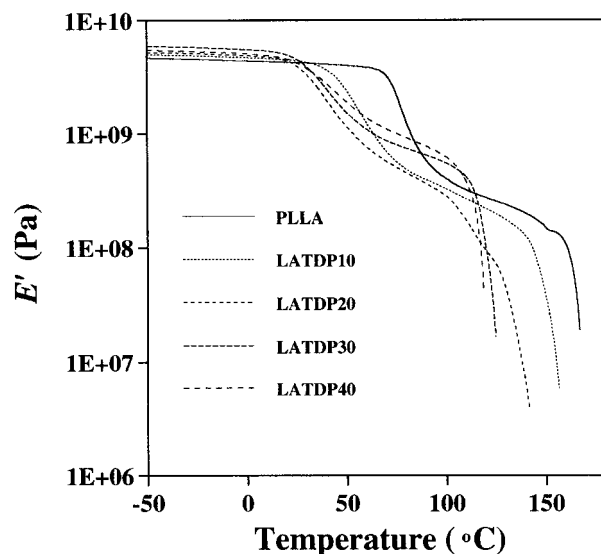


Figure 12 The storage modulus (E') of pure PLLA and PLLA/TDP blends with TDP contents from 0 to 40 wt %, which was measured at 5 Hz and with a heating rate of $2^{\circ}C/min$. The samples were aged at $70^{\circ}C$ for 1 week.

Mechanical Properties

The modulus, stress, and strain of the hot-pressed films annealed at $70^{\circ}C$ for 1 week and aged at room temperature for 2 months are listed in Table II. For the sample aged at room temperature, the E of the LATDP10 blend was larger than that of pure PLLA while the stress at the maximum point (σ_m) was smaller than that of PLLA. As for the LATDP30 blend, the tensile parameters E and σ_m were much lower than those of PLLA and the LATDP10 blend. However, the strain at break (ϵ_b) of LATDP30 was about 50 times as high as that of PLLA. These results suggested that TDP greatly modified the mechanical properties of PLLA.

The thermal history also affected the properties of the PLLA/TDP blend. The ϵ_b of LATDP30

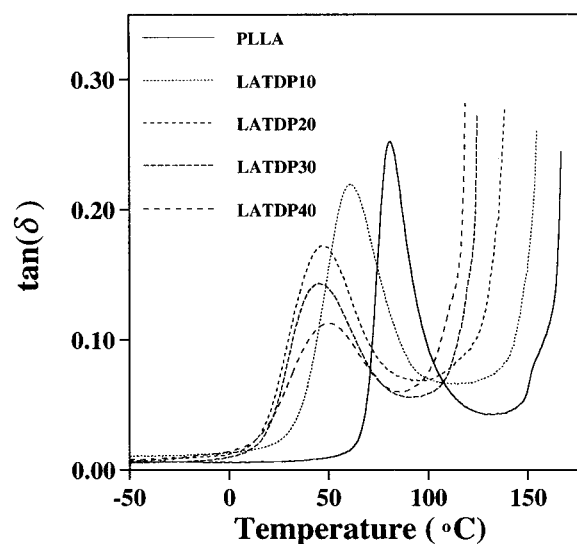


Figure 13 The loss tangent $\tan(\delta)$ of pure PLLA and PLLA/TDP blends with TDP contents from 0 to 40% measured at 5 Hz and with a heating rate of $2^{\circ}C/min$.

aged at room temperature was $470 \pm 70\%$ while that annealed at $70^{\circ}C$ was $2.5 \pm 0.3\%$. The glass transition of LATDP30 was $36^{\circ}C$, close to room temperature. For the LATDP30 sample aged at room temperature the melting enthalpy was small ($11.1 J/g$, Table I), and it could be roughly regarded as an elastomer at room temperature. Thus, LATDP30 possessed very high ϵ_b in this case. For the LATDP30 blend annealed at $70^{\circ}C$ the melting enthalpy was large ($43.3 J/g$, Table I). In this case the LATDP30 blend was brittle plastic and the σ_b was very low.

Effect of Chemical Structure of Small Molecule on Thermal Properties of Blend

In this study, the thermal properties of PLLA blends with DPM, CAT, DHB, DHEB, and HDO were also investigated by DSC. Similar to TDP,

Table II Modulus (E), Stress (σ_m), and Strain (ϵ_b) of PLLA/TDP Samples Aged at $70^{\circ}C$ or Room Temperature (RT)

Sample	$70^{\circ}C$ for 1 Week			RT for 2 Months		
	E (MPa)	σ_m (MPa)	ϵ_b (%)	E (MPa)	σ_m (MPa)	ϵ_b (%)
PLLA	1770 ± 180	58 ± 8	6.8 ± 3.0	1470 ± 160	57 ± 7	10 ± 3
LATDP10	1847 ± 50	49 ± 8	5.0 ± 1.0	2000 ± 260	46 ± 2	5.8 ± 0.7
LATDP20	1490 ± 90	31 ± 6	6.1 ± 2.0	1490 ± 90	38 ± 4	4.6 ± 1.0
LATDP30	—	9.5 ± 1.4	2.5 ± 0.3	—	5.4 ± 1.6	470 ± 70

all these low molecular weight molecules contain two hydroxyl groups at the molecular terminuses.

The melting points of these blends (cast films aged at 70°C for more than 1 week) determined from the DSC curves are summarized in Figure 14. Obviously, the melting point of PLLA decreased after the addition of low molecular weight compounds. In addition, it can be seen that the variations of the melting points with additive content in PLLA/TDP, PLLA/DPM, PLLA/DHB, and PLLA/CAT blends were larger than those in PLLA/HDO and PLLA/DHEB blends (Fig. 14). Similar results can also be observed in Figure 15 for the T_g . These facts suggested that dihydric phenol (TDP, DPM, DHB, and CAT) significantly modified and dihydric alcohol (DHEB or HDO) insignificantly modified the thermal properties of PLLA.

CONCLUSIONS

As detected by FTIR, intermolecular hydrogen bonds were formed between the PLLA chain and TDP molecule in the blends aged at room temperature. The fractions of the associated carbonyl group F_b values were found to increase with the TDP content.

The thermal analysis revealed that PLLA/TDP blends possessed eutectic phase behavior. The

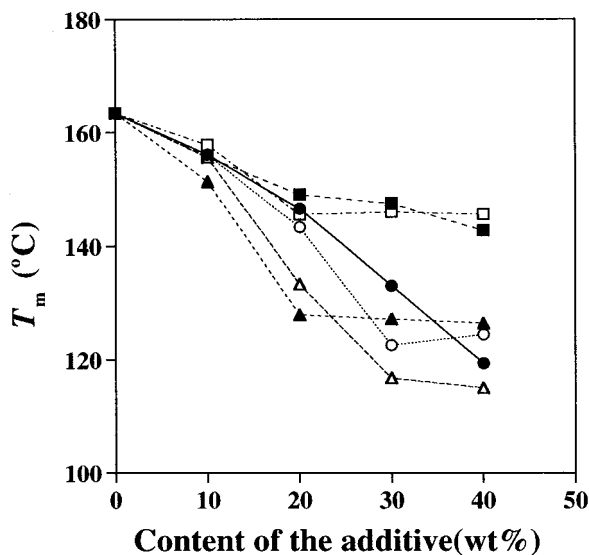


Figure 14 The melting points (T_m) of PLLA blends with various low molecular weight compounds. (●) PLLA/TDP, (○) PLLA/DPM, (▲) PLLA/DHB, (△) PLLA/CAT, (■) PLLA/DHEB, and (□) PLLA/HDO.

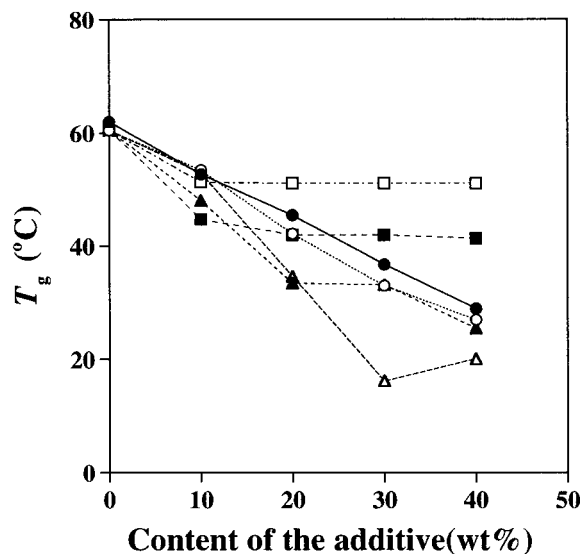


Figure 15 The glass-transition temperatures (T_g) of PLLA blends with various low molecular weight compounds. (●) PLLA/TDP, (○) PLLA/DPM, (▲) PLLA/DHB, (△) PLLA/CAT, (■) PLLA/DHEB, and (□) PLLA/HDO.

thermal and mechanical properties of PLLA were greatly modified through blending with TDP. The melting points and the glass-transition temperatures of PLLA decreased with the increase of TDP content. At the α -transition peak of the DMTA spectra, the loss tangent $\tan(\delta)$ of the blends also decreased after the addition of TDP. The formation of hydrogen bonds and the thermal and mechanical properties of PLLA/TDP blends were strongly dependent on the thermal history. The thermal analysis on the blends of PLLA with different low molecular weight compounds suggested that dihydric phenols but not dihydric alcohol were effective for modification of the properties of PLLA.

The authors are grateful to Mitsui Chemical, Inc., for kindly supplying the poly(L-lactic acid) sample.

REFERENCES

1. Mayer, J. M.; Kaplan, D. L. *Trends Polym Sci* 1994, 2, 227.
2. Heller, J. *Biomaterials* 1980, 1, 51.
3. Vainionpaa, S.; Rokkanen, P.; Tormala, P. *Prog Polym Sci* 1989, 14, 679.
4. Pennings, J. P.; Dijkstra, H.; Pennings, A. J. *Polymer* 1993, 34, 942.

5. Leenslag, J. W.; Pennings, A. J.; Bos, R. M.; Rozema, F. R.; Boering, G. *Biomaterials* 1987, 8, 311.
6. Gu, J. D.; Gada, M.; Kharas, G.; Eberiel, D.; McCarthy, S. P.; Gross, R. A. *Polym Mater Sci Eng* 1992, 67, 351.
7. Cha, Y.; Pitt, C. G. *Biomaterials* 1990, 11, 108.
8. Yoon, J. S.; Oh, S. H.; Kim, M. N.; Chin, I. J.; Kim, Y. H. *Polymer* 1999, 40, 2303.
9. Zhang, L. L.; Goh, S. H.; Lee, S. Y. *J Appl Polym Sci* 1998, 70, 811.
10. Gan, Z.; Yu, D.; Zhong, Z.; Liang, Q.; Jing, X. *Polymer* 1999, 40, 2859.
11. Tsuji, H.; Mizuno, A.; Ikada, Y. *J Appl Polym Sci* 1998, 70, 2259.
12. Koyama, N.; Doi, Y. *Polymer* 1997, 38, 1589.
13. Nijenhuis, A. J.; Colstee, E.; Grijpma, D. W.; Pennings, A. J. *Polymer* 1996, 37, 5849.
14. Labbecque, L. V.; Kumar, R. A.; Dave, V.; Gross, R. A.; McCarthy, S. P. *J Appl Polym Sci* 1997, 66, 1507.
15. Wu, C.; Yamagishi, T.; Nakamoto, Y.; Ishida, S. *Polymer Prepr Jpn* 1999, 48, 4167.
16. He, Y.; Asakawa, N.; Inoue, Y. *J Polym Sci Part B: Polym Phys* 2000, 38, 1848.
17. Iriondo, P.; Iruin, J. J.; Fernandez-Berridi, M. J.; *Macromolecules* 1996, 29, 5605.
18. Li, D.; Brisson, J. *Polymer* 1998, 39, 801.
19. Li, D.; Brisson, J. *Polymer* 1998, 39, 793.
20. Coleman, M. M.; Graf, J. F.; Painter, P. C. *Specific Interactions and the Miscibility of Polymer Blends*; Technomic Publishing Co.: Lancaster, PA, 1991.
21. Belfiore, L. A.; Ueda, E. *Polymer* 1992, 33, 3833.
22. Smith, P.; Pennings, A. J. *Polymer* 1974, 15, 413.
23. Paternostre, L.; Damman, P.; Dosiere, M. *Macromolecules* 1999, 32, 153.